Available online at www.sciencedirect.com
SCIENCE DIRECT®
ELSEVIER
International Journal of Solids and Structures 42 (2005) 5010–5020
INTERNATIONAL JOURNAL OF SOLIDS and STRUCTURES
www.elsevier.com/locate/ijsolstr

A new integral equation formulation of two-dimensional inclusion–crack problems

C.Y. Dong [a,*], Kang Yong Lee [b]

[a] *Department of Applied Mechanics, Beijing Institute of Technology, Beijing 100081, China*
[b] *School of Mechanical Engineering, Yonsei University, Seoul 120-749, Korea*

Received 15 September 2004; received in revised form 12 February 2005
Available online 29 March 2005

Abstract

A new integral equation formulation of two-dimensional infinite isotropic medium (matrix) with various inclusions and cracks is presented in this paper. The proposed integral formulation only contains the unknown displacements on the inclusion–matrix interfaces and the discontinuous displacements over the cracks. In order to solve the inclusion–crack problems, the displacement integral equation is used when the source points are acting on the inclusion–matrix interfaces, whilst the stress integral equation is adopted when the source points are being on the crack surfaces. Thus, the resulting system of equations can be formulated so that the displacements on the inclusion–matrix interfaces and the discontinuous displacements over the cracks can be obtained. Based on one point formulation, the stress intensity factors at the crack tips can be achieved. Numerical results from the present method are in excellent agreement with those from the conventional boundary element method.

Keywords: Integral equation; Isotropic medium; Inclusions; Cracks

1. Introduction

Heterogeneous materials often contain various inclusions (voids can be taken as the special inclusions with zero elastic modulus) and cracks. The interaction between the inclusions and the cracks can be analyzed using various numerical methods such as the finite element method (Zienkiewicz, 1989) and the boundary element method (Aliabadi, 2002; Brebbia and Dominguez, 1992; Brebbia et al., 1984).

* Corresponding author.
E-mail addresses: chunyingdong@yahoo.com (C.Y. Dong), kyl2813@yonsei.ac.kr (K.Y. Lee).

0020-7683/$ - see front matter © 2005 Elsevier Ltd. All rights reserved.
doi:10.1016/j.ijsolstr.2005.02.019

Application of the finite element method in heterogeneous materials can be found in many references, e.g. Thomson and Hancock (1984), Ghosh and Mukhopadhyay (1993) and Barsoum (1976). Considering the geometric irregularity of the inclusions, the randomness of the inclusion distribution and various cracks, it is not easy to carry out mesh division and to simulate the crack propagation. The interaction between a circular inclusion and an arbitrarily oriented crack has been investigated using an integral equation method (Erdogan et al., 1974). An integral equation method was also used to analyze the interaction between an elastic circular inclusion and two symmetric collinear cracks (Hsu and Shivakumar, 1976). Crack propagation simulation of the crack–inclusion plate was investigated using the body force method (Saimoto and Nisitani, 1998). However, these researches were only limited to the inclusions with simple geometry such as circular and elliptical inclusions. Interaction between various coated inclusions and cracks has been investigated using the boundary element method and the domain integral equation method (Dong et al., 2003a). In the boundary element method, the interface condition, i.e. displacement continuity and traction equilibrium, has been used to formulate the resulting system of equations. In the domain integral equation method, only the isotropic matrix fundamental solution for anisotropic inclusions is used so that the complex fundamental solution for anisotropic medium can be avoided. The price paid is that the inclusions have to discretized into some finite elements. The domain integral equation method was also used to investigate the propagation of the crack near the inclusion (Dong et al., 2003b) and 3D inclusion–crack interaction (Dong et al., 2002).

In this paper, based on the methods proposed by Leite et al. (2003) for two-dimensional reinforced solid and Dong and de Pater (2001) for hydraulic fracturing, a new integral equation formulation is presented to solve two-dimensional inclusion–crack problems. Compared with the conventional boundary element method for the inclusion–crack problems, the present integral equation formulation only contains the displacements (no tractions) on the inclusion–matrix interfaces and the discontinuous displacements over the cracks. Similar to the domain integral equation approach, the present integral equation approach can also avoid the corner node problems (due to different normal directions at the corner nodes), thus irregular inclusion shapes can easily be dealt with. In order to accurately calculate the stress intensity factors at the crack tips, special crack tip elements (Dong and de Pater, 2001) are used to model the $\sqrt{r}$ variation of the displacements near the crack tips. Numerical examples are presented to show the validity and the effectiveness of the present method.

2. Basic formulation

For the cracked infinite isotropic matrix subjected to remote stresses, the displacement and the stress integral equations at the point P being in the matrix can be given as follows (Dong et al., 2003a):

$$u_k(P) = u_k^0(P) + \int_\Gamma U_{ki}(P,q)t_i(q)\,\mathrm{d}\Gamma(q) - \int_\Gamma T_{ki}(P,q)u_i(q)\,\mathrm{d}\Gamma(q) + \int_{\Gamma_c} T_{ki}(P,q)D_i(q)\,\mathrm{d}\Gamma \tag{1}$$

and

$$\sigma_{kl}(P) = \sigma_{kl}^0(P) + \int_\Gamma U_{kli}(P,q)t_i(q)\,\mathrm{d}\Gamma(q) - \int_\Gamma T_{kli}(P,q)u_i(q)\,\mathrm{d}\Gamma(q) + \int_{\Gamma_c} T_{kli}(P,q)D_i(q)\,\mathrm{d}\Gamma \tag{2}$$

where q is the field point acting on the problem boundary. Γ and Γ_c denote the inclusion–matrix interface and the crack surface, respectively. u_k^0 and σ_{kl}^0 are, respectively, the displacements and the stresses at the point P caused by remote stresses in an infinite homogeneous isotropic elastic matrix. $D_i(q) = u_i(q^-) - u_i(q^+)$ in which q^- and q^+ are two points having the same coordinates of the lower and the upper surfaces of the crack. U_{ki}, T_{ki}, U_{kli} and T_{kli} are the fundamental solutions of an infinite isotropic elastic medium which are as follows (Brebbia and Dominguez, 1992):

$$U_{ki} = \frac{1}{8\pi G(1-v)}\left[(3-4v)\ln\left(\frac{1}{r}\right)\delta_{ki} + \frac{\partial r}{\partial x_k}\frac{\partial r}{\partial x_i}\right] \tag{3a}$$

$$T_{ki} = -\frac{1}{4\pi(1-v)r}\left[\frac{\partial r}{\partial n}\left\{(1-2v)\delta_{ki} + 2\frac{\partial r}{\partial x_k}\frac{\partial r}{\partial x_i}\right\} - (1-2v)\left(\frac{\partial r}{\partial x_k}n_i - \frac{\partial r}{\partial x_i}n_k\right)\right] \tag{3b}$$

$$U_{kli} = \frac{1}{4\pi(1-v)r}\{(1-2v)[\delta_{ki}r_{,l} + \delta_{li}r_{,k} - \delta_{kl}r_{,i}] + 2r_{,i}r_{,l}r_{,k}\} \tag{3c}$$

$$\begin{aligned} T_{kli} = \frac{G}{2\pi(1-v)r^2}\Bigg\{ & 2\frac{\partial r}{\partial n}[(1-2v)\delta_{kl}r_{,i} + v(\delta_{ki}r_{,l} + \delta_{li}r_{,k}) - 4r_{,i}r_{,l}r_{,k}] \\ & + 2v(n_k r_{,i}r_{,l} + n_l r_{,i}r_{,k}) + (1-2v)(2n_i r_{,k}r_{,l} + n_k\delta_{li} + n_l\delta_{ki}) - (1-4v)n_i\delta_{kl}\Bigg\} \end{aligned} \tag{3d}$$

where δ_{kl} is the Kronecker delta. $r_{,i} = \frac{\partial r(P,q)}{\partial x_i(q)}$ in which r is the distance between the field point q and the source point P. $\frac{\partial r}{\partial n} = r_{,i}n_i$ in which n_i is the directional cosine of the normal at the boundary point q with respect to x_i. G and v are shear modulus and Poisson's ratio, respectively.

When the source point P approaches the boundary point p being on the inclusion–matrix interface, Eq. (1) becomes

$$c_{ki}u_i(p) = u_k^0(p) + \int_\Gamma U_{ki}(p,q)t_i(q)\,\mathrm{d}\Gamma(q) - \int_\Gamma^{\mathrm{c}} T_{ki}(p,q)u_i(q)\,\mathrm{d}\Gamma(q) + \int_{\Gamma_\mathrm{c}} T_{ki}(p,q)D_i(q)\,\mathrm{d}\Gamma \tag{4}$$

where c_{ki} depends on the boundary geometry at the source point p. The symbol $\int^{\mathrm{c}}$ denotes the Cauchy principal value integral.

When the source point P arrives at the point p over the crack surface, the stress integral equation becomes

$$\sigma_{kl}(p) = \sigma_{kl}^0(p) + \int_\Gamma U_{kli}(p,q)t_i(q)\,\mathrm{d}\Gamma(q) - \int_\Gamma T_{kli}(p,q)u_i(q)\,\mathrm{d}\Gamma(q) + \int_{\Gamma_\mathrm{c}}^{\mathrm{s}} T_{kli}(p,q)D_i(q)\,\mathrm{d}\Gamma \tag{5}$$

where $\int^{\mathrm{s}}$ represents the Hadamard finite-part integral.

For the Ith isotropic inclusion, the corresponding displacement boundary integral equation can be given as (Brebbia and Dominguez, 1992)

$$c_{ki}^I(p)u_i^I(p) = \int_{\Gamma_I} U_{ki}^I(p,q)t_i^I(q)\,\mathrm{d}\Gamma(q) - \int_{\Gamma_I}^{\mathrm{c}} T_{ki}^I(p,q)u_i^I(q)\,\mathrm{d}\Gamma(q) \tag{6}$$

where Γ_I represents the Ith inclusion–matrix interface.

From Eqs. (3a) to (3d), and assuming that there is the same Poisson's ratio for the matrix and the inclusions, one can find the following relationships (Leite et al., 2003):

$$U_{ki}^I = \frac{G}{G^I}U_{ki} \tag{7a}$$

$$T_{ki}^I = T_{ki} \tag{7b}$$

$$U_{kli}^I = U_{kli} \tag{7c}$$

$$T_{kli}^I = \frac{G^I}{G}T_{kli} \tag{7d}$$

Substituting (7a) and (7b) into Eq. (6), then adding Eqs. (4) and (6) and considering the interface conditions, one can obtain the following displacement boundary integral equation:

$$c_{ki}\left(1+\frac{G^I}{G}\right)u_i(p)=u_i^0(p)-\int_{\Gamma_I}^{c}\left(1-\frac{G^I}{G}\right)T_{ki}(p,q)u_i(q)\,\mathrm{d}\Gamma+\int_{\Gamma_c}T_{ki}(p,q)D_i(q)\,\mathrm{d}\Gamma \tag{8}$$

For the matrix with multiple inclusions and cracks, Eq. (8) can be extended to the following form:

$$\begin{aligned}c_{ki}\left(1+\frac{G^I}{G}\right)u_i(p)=u_i^0(p)&-\int_{\Gamma_I}^{c}\left(1-\frac{G^I}{G}\right)T_{ki}(p,q)u_i(q)\,\mathrm{d}\Gamma\\&-\sum\nolimits_{J=1,\neq I}^{\mathrm{NI}}\int_{\Gamma_J}\left(1-\frac{G^J}{G}\right)T_{ij}(p,q)u_j(q)\,\mathrm{d}\Gamma+\sum\nolimits_{c=1}^{\mathrm{NC}}\int_{\Gamma_c}T_{ki}(p,q)D_i(q)\,\mathrm{d}\Gamma\end{aligned} \tag{9}$$

where NI and NC denote the numbers of the inclusions and the cracks, respectively. The source point p is acting on the Ith inclusion–matrix interface.

Similarly, the stress integral equation for the point p being on the ICth crack surface can be written as

$$\begin{aligned}\sigma_{kl}(p)=\sigma_{kl}^0(p)&-\sum_{I=1}^{\mathrm{NI}}\int_{\Gamma_I}\left(1-\frac{G^I}{G}\right)T_{kli}(p,q)u_i(q)\,\mathrm{d}\Gamma+\int_{\Gamma_{\mathrm{IC}}}^{s}T_{kli}(p,q)D_i(q)\,\mathrm{d}\Gamma\\&+\sum_{JC=1,\neq\mathrm{IC}}^{\mathrm{NC}}\int_{\Gamma_{JC}}T_{kli}(p,q)D_i(q)\,\mathrm{d}\Gamma\end{aligned} \tag{10}$$

From Eqs. (9) and (10), one can find that the displacement and the stress boundary integral equations only contain the displacements on the inclusion–matrix interfaces and the discontinuous displacements over the crack surfaces. Note that the tractions on the inclusion–matrix interfaces disappear in these two integral equations. Therefore, contrary to the conventional boundary element method in which discontinuous elements are used near the corners of irregular inclusions (Dong et al., 2003c), arbitrary inclusion shapes can be easily dealt with using Eqs. (9) and (10). If there are no any cracks in the matrix, Eqs. (9) and (10) will reduce to the equations presented by Leite et al. (2003).

In numerical implementation, quadratic boundary elements are used to discretize the inclusion–matrix interfaces, whilst a series of discontinuous quadratic boundary elements are employed to mesh the cracks. Special crack tip elements (Dong and de Pater, 2001) are used to model the $\sqrt{r}$ variation of the displacements near the crack tips. For the source point p being on the inclusion–matrix interface, Eq. (9) is used, whilst for the source point p being on the crack surface, Eq. (10) is adopted. Through these processes, a resulting system of equations can be obtained as follows:

$$\begin{bmatrix}A_{11} & A_{12}\\ A_{21} & A_{22}\end{bmatrix}\begin{Bmatrix}\mathbf{U}\\ \mathbf{D}\end{Bmatrix}=\begin{Bmatrix}\widetilde{\mathbf{U}}\\ \widetilde{\boldsymbol{\sigma}}\end{Bmatrix} \tag{11}$$

where A_{ij} is the related coefficient matrix from Eqs. (9) and (10). $\mathbf{U}$ and $\mathbf{D}$ are the vectors of the displacements on the inclusion–matrix interfaces and the discontinuous displacements over the crack surfaces, respectively. $\widetilde{\mathbf{U}}$ is the vector of the displacements on the inclusion–matrix interfaces caused by remote stresses, whilst $\widetilde{\boldsymbol{\sigma}}$ is the vector of the stresses caused by remote stresses and the pressure acting on the crack surfaces.

Once the discontinuous displacements over the crack surfaces are available, the stress intensity factors can be calculated by one point formulation, i.e. (Shou and Crouch, 1995)

$$K_I=\frac{G}{4(1-\nu)}\sqrt{\frac{2\pi}{r}}D_n(r) \tag{12}$$

and

$$K_{II}=\frac{G}{4(1-\nu)}\sqrt{\frac{2\pi}{r}}D_s(r) \tag{13}$$

where r is the distance from the crack tip. D_n and D_s are the normal and the shear components of discontinuous displacements over the cracks, respectively.

3. Numerical examples

3.1. An infinite isotropic elastic medium (matrix) containing one cylindrical elastic inclusion and one crack

One cylindrical elastic inclusion and one radially oriented crack are embedded into an infinite isotropic elastic medium subjected to a remote unit stress σ^0 as shown in Fig. 1. This problem has been investigated by some researchers, e.g. Lam et al. (1998) and Dong et al. (2003b). The aim of choosing this problem is to check numerical accuracy of the present method. The Poisson's ratios of both the inclusion and the matrix are respectively taken as 0.25. The crack length $2a$ and the cylindrical inclusion radius R are assumed to be 1, respectively. The inclusion–matrix interface is discretized into 16 quadratic boundary elements, whilst the crack surface is meshed into 20 quadratic discontinuous elements.

Fig. 2 shows the variation of the stress intensity factor at crack tip A for soft materials with the distance d between the crack and the inclusion. For $G_i/G = 0.0$ and 0.5, the results from the present method are in

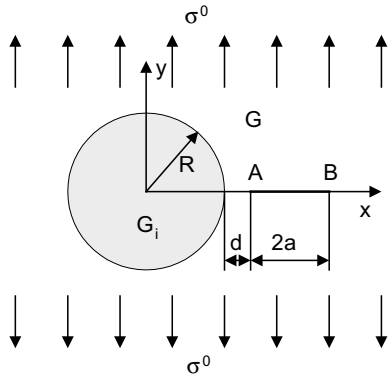

Fig. 1. Cylindrical inclusion–crack configuration.

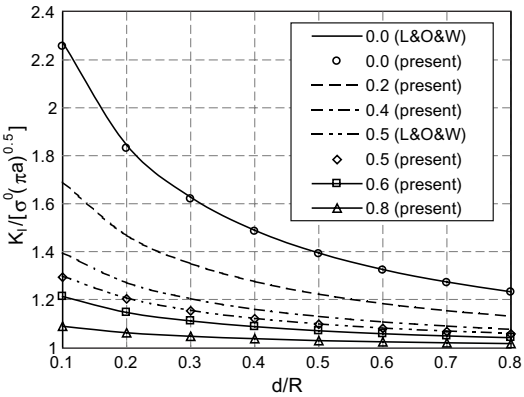

Fig. 2. Stress intensity factor at crack tip A for different inclusion materials (the number in the legend denotes the value of $G_i/G < 1.0$).

excellent agreement with those given by Lam et al. (1998). For other soft inclusions, the corresponding results from the present method are also shown in Fig. 2. One can find that the non-dimensional stress intensity factor at crack tip A is always over 1 for soft inclusions. With the increase of the distance d between the crack and the inclusion, the stress intensity factor at crack tip A decreases. Compared with other soft inclusions, void leads to the largest variation of the stress intensity factor at crack tip A. The stress intensity factor for hard inclusion is shown in Fig. 3. Similar to the soft inclusion case, one can also observe that the results from the present method are in excellent agreement with those by Lam et al. (1998). The non-dimensional stress intensity factor at crack tip A for hard inclusion is always below 1. Relative to other hard inclusions, rigid inclusion leads to the lowest value of the stress intensity factor at crack tip A.

3.2. One equilateral hexagonal inclusion and two cracks embedded in an infinite isotropic elastic medium

One equilateral hexagonal inclusion and two symmetrical cracks are embedded in an infinite isotropic elastic medium subjected to a remote unit loading σ^0 as shown in Fig. 4. The Poisson's ratios of both the inclusion and the matrix are respectively taken as 0.25. Each edge length of the equilateral hexagonal inclusion is equal to 1. The crack length $2a$ is taken as 1. The distance d is chosen to be 0.1.

Each edge of the equilateral hexagonal inclusion is meshed into six quadratic boundary elements, in which two discontinuous boundary elements near two corners of each edge are used for the conventional boundary element method (Dong et al., 2003c). The cracks AB and CD are respectively discretized into 20

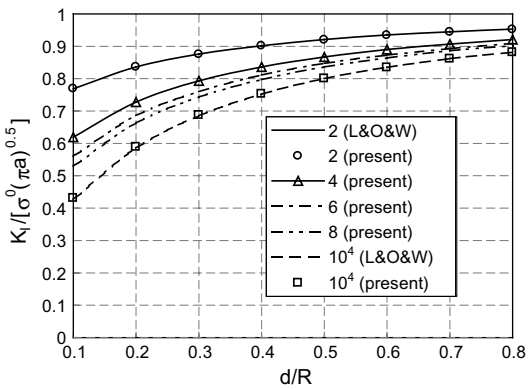

Fig. 3. Stress intensity factor at crack tip A for different inclusion materials (the number in the legend denotes the value of $G_i/G > 1.0$).

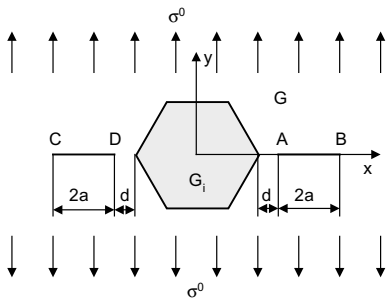

Fig. 4. Equilateral hexagonal inclusion—two symmetrical cracks.

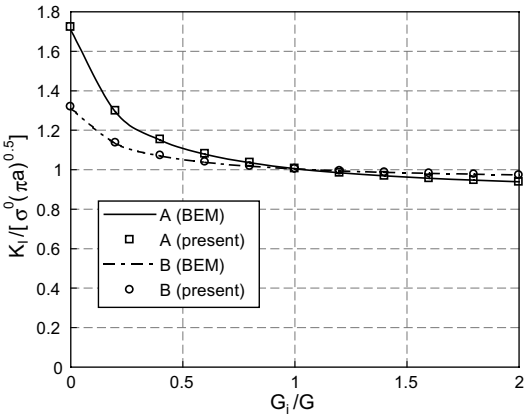

Fig. 5. Stress intensity factor at crack tips A and B for different inclusion materials G_i/G.

quadratic discontinuous elements. For different values of G_i/G, the stress intensity factors at the crack tips A and B or D and C from the conventional boundary element method and the present method are shown in Fig. 5. One can observe that two methods produce almost the same results. For $G_i/G < 1.0$ ($G_i/G > 1.0$), the non-dimensional stress intensity factors at crack tips A and B are always bigger (smaller) than 1.

3.3. One cylindrical inclusion, one crack and one void embedded in an infinite isotropic elastic medium

One cylindrical inclusion, one crack and one void are embedded in an infinite isotropic elastic medium subjected to a remote unit loading σ^0 as shown in Fig. 6. The Poisson's ratios of both the inclusion and the matrix are respectively taken as 0.25. The distances CA and BD are respectively assumed to be 0.1. The radii, R, of the inclusion and the void are equal to 1, respectively. The centers of the inclusion and the void are respectively situated at O_1 $(-1.6, 0)$ and O_2 $(1.6, 0)$. The crack length $2a$ is taken as 1.

This example has been solved using the domain integral equation method (Dong et al., 2003b). In the present analysis, the conventional boundary element method and the present method are respectively used to solve this example. The crack AB is discretized into 20 quadratic discontinuous elements. The inclusion–matrix interface and the void boundary are respectively meshed into 16 quadratic boundary elements. For different values of G_i/G, the stress intensity factors at the crack tips A and B from the conventional boundary element method and the present method are shown in Fig. 7. It can be found that excellent agreement between the results from two methods has been obtained. With the increase of G_i/G, the stress intensity

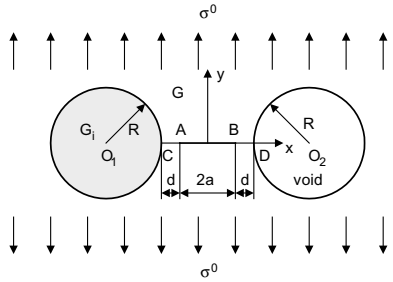

Fig. 6. Inclusion–crack–void configuration.

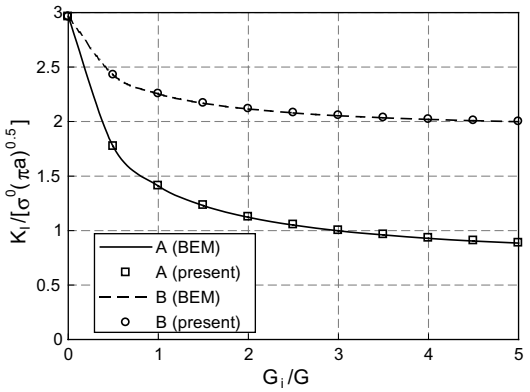

Fig. 7. Stress intensity factor at crack tips A and B for different inclusion materials G_i/G.

factors at crack tips A and B decreases. When $G_i/G = 10^3$, the non-dimensional stress intensity factors at crack tips A and B are 0.684 and 1.896 (0.675 and 1.896 for the conventional boundary element method), respectively.

3.4. One equilateral triangle inclusion, one crack and one equilateral triangle void embedded in an infinite isotropic elastic medium

One equilateral triangle inclusion, one crack and one equilateral triangle void are embedded in an infinite isotropic elastic medium subjected to a remote unit loading σ^0 as shown in Fig. 8. The Poisson's ratios of both the inclusion and the matrix are respectively taken as 0.25. The distances CA and BD are respectively assumed to be 0.1. Each edge length of the equilateral triangle inclusion and the equilateral triangle void is equal to 1. The crack length $2a$ is taken as 1.

Similar to the above examples, the conventional boundary element method (Dong et al., 2003c) and the present method are used to study this example. The crack AB is discretized into 20 quadratic discontinuous elements. Each edge of the equilateral triangle inclusion and the equilateral triangle void is meshed into six quadratic boundary elements, in which two discontinuous boundary elements near two corners of each edge are used for the conventional boundary element method. For different values of G_i/G, the stress intensity factors at the crack tips A and B from the conventional boundary element method and the present

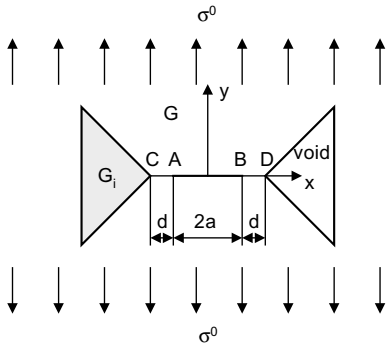

Fig. 8. Equilateral triangle inclusion–crack–equilateral triangle void configuration.

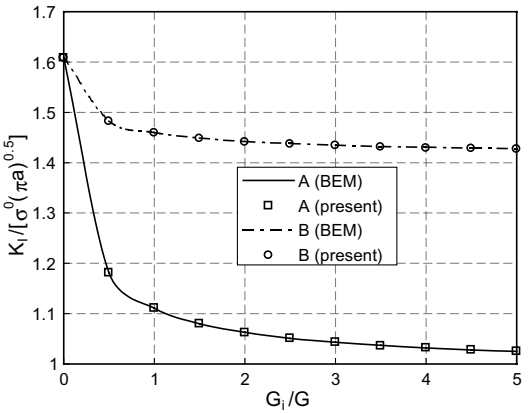

Fig. 9. Stress intensity factor at crack tips A and B for different inclusion materials G_i/G.

method are shown in Fig. 9. One can find that almost the same results from two methods have been obtained. When $G_i/G = 10^3$, the non-dimensional stress intensity factors at crack tips A and B are 0.997 and 1.415 (0.998 and 1.417 for the conventional boundary element method), respectively.

3.5. One square inclusion, one crack and one square void embedded in an infinite isotropic elastic medium

One square inclusion, one crack and one square void are embedded in an infinite isotropic elastic medium subjected to a remote unit loading σ^0 as shown in Fig. 10. The Poisson's ratios of both the inclusion and the matrix are respectively taken as 0.25. The distances CA and BD are respectively assumed to be 0.1. Each edge length of the square inclusion and the square void is equal to 1. The centers of the square inclusion and the square void are respectively situated at $(-1.6, 0)$ and $(1.6, 0)$. The crack length $2a$ is taken as 1.

Similar to the above examples, the crack AB is discretized into 20 quadratic discontinuous elements. Each edge of the square inclusion and the square void is meshed into six quadratic boundary elements, in which two discontinuous boundary elements near two corners of each edge are used for the conventional boundary element method (Dong et al., 2003c). For different values of G_i/G, the stress intensity factors at the crack tips A and B from the conventional boundary element method and the present method are shown in Fig. 11. It can be found that two methods lead to almost the same results. When $G_i/G = 10^3$, the

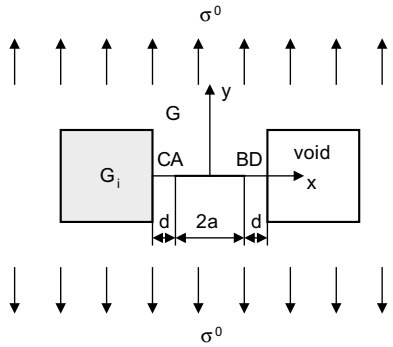

Fig. 10. Square inclusion–crack–square void configuration.

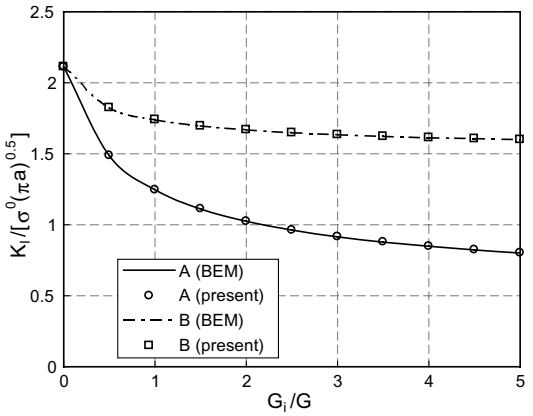

Fig. 11. Stress intensity factor at crack tips A and B for different inclusion materials G_i/G.

non-dimensional stress intensity factors at crack tips A and B are 0.519 and 1.508 (0.520 and 1.508 for the conventional boundary element method), respectively.

4. Conclusions

A new integral equation approach has been presented to solve various inclusion–crack problems. The present integral equation formulation only contains the displacements on the inclusion–matrix interfaces and the discontinuous displacements over the crack surfaces. In the conventional boundary element method in which for the matrix and the inclusions, their respective integral equations must be formulated, then the interface conditions (displacement continuity and traction equilibrium) have to be enforced. Specially, for irregular inclusions, the discontinuous elements near corners are used to avoid the corner problem. However, the present integral equation does not contain the interface-matrix traction, therefore there is no the corner problem. Various inclusion–crack problems are easily to be solved using the present method. Numerical results are in excellent agreement with those from the conventional boundary element method.

Acknowledgement

CY Dong is grateful for the support provided by a Brain Pool grant from the Korea Science and Engineering Foundation (KOSEF).

References

Aliabadi, M.H., 2002. The Boundary Element Method—Applications in Solids and Structures. John Wiley and Sons.

Barsoum, R.S., 1976. On the use of isoparametic finite elements in linear fracture mechanics. Int. J. Num. Meth. Eng. 10, 25–37.

Brebbia, C.A., Dominguez, J., 1992. Boundary Elements—An Introduction Course. Computational Mechanics Publications, New York.

Brebbia, C.A., Telles, J.C.F., Wrobel, L.C., 1984. Boundary Element Techniques—Theory and Applications in Engineering. Springer, Berlin.

Dong, C.Y., Lo, S.H., Cheung, Y.K., 2003a. Interaction between coated inclusions and cracks in an infinite isotropic elastic medium. Eng. Anal. Bound. Elem. 27, 871–884.

Dong, C.Y., Lo, S.H., Cheung, Y.K., 2003b. Numerical analysis of the inclusion–crack interactions using an integral equation. Comput. Mech. 30, 119–130.

Dong, C.Y., Lo, S.H., Cheung, Y.K., 2003c. Stress analysis of inclusion problems of various shapes in an infinite anisotropic elastic medium. Comput. Meth. Appl. Mech. Eng. 192, 683–696.

Dong, C.Y., de Pater, C.J., 2001. Numerical implementation of displacement discontinuity method and its application in hydraulic fracturing. Comput. Meth. Appl. Mech. Eng. 191, 745–760.

Dong, C.Y., Cheung, Y.K., Lo, S.H., 2002. An integral equation approach to the inclusion–crack interactions in three-dimensional infinite elastic domain. Comput. Mech. 29, 313–321.

Erdogan, F., Gupta, G.D., Ratwani, M., 1974. Interaction between a circular inclusion and an arbitrarily oriented crack. ASME J. Appl. Mech. 41, 1007–1011.

Ghosh, S., Mukhopadhyay, S.N., 1993. A material based finite element analysis of heterogeneous media involving Dirichlet tessellations. Comput. Meth. Appl. Mech. Eng. 104, 211–247.

Hsu, Y.C., Shivakumar, V., 1976. Interaction between an elastic circular inclusion and two symmetrically placed collinear cracks. Int. J. Fract. 12, 619–630.

Lam, K.Y., Ong, P.P., Wude, N., 1998. Interaction between a circular inclusion and a symmetrically branched crack. Theor. Appl. Fract. Mech. 28, 197–211.

Leite, L.G.S., Coda, H.B., Venturini, W.S., 2003. Two-dimensional solids reinforced by thin bars using the boundary element method. Eng. Anal. Bound. Elem. 27, 193–201.

Saimoto, A., Nisitani, H., 1998. Crack propagation simulation in a plate with cracks and inclusion. In: Brebbia, C.A., Carpinteri, A. (Eds.), Damage and Fracture Mechanics. Computational Mechanics Publications, Southampton, UK, pp. 3–12.

Shou, K.J., Crouch, S.L., 1995. A higher order displacement discontinuity method for analysis of crack problems. Int. J. Rock Mech. Min. Sci. Geomech. Abstr. 32 (1), 49–55.

Thomson, R.D., Hancock, J.W., 1984. Local stress and strain fields near a spherical elastic inclusion in a plastically deforming matrix. Int. J. Fract. 24, 209–228.

Zienkiewicz, O.C., 1989. The Finite Element Method, fourth ed. McGraw-Hill, London.